

Finite Element Analysis of Axially Loaded GFRP-Reinforced Concrete Hollow Square Columns

Hussein A. Hussein^{1, a*} and AbdulMuttalib I. Said^{1, b}

¹Civil Engineering Department, University of Baghdad, Baghdad, Iraq

^ahussein.hussein2001m@coeng.uobaghdad.edu.iq and ^bdr.abdulmuttalib.i.said@coeng.uobaghdad.edu.iq

*Corresponding author

Abstract. Hollow concrete columns are often employed in bridge constructions because of their lighter weight and effective section characteristics. In addition, to reduce the issue of steel reinforcement corrosion and create a strong and light construction, hollow section columns are also reinforced with bars made of fiber-reinforced polymer. This research aimed to analyze the effect of GFRP (glass fiber reinforced polymer) on the compression strength of hollow square concrete columns under an axial concentric load. The finite element application ABAQUS 2019 version was used to simulate a finite element model, calibrated utilizing experimental data from previous studies for various geometric models of concrete and material specifications of the reinforcement. The findings of the experimental studies and the finite element model exhibit excellent agreement. Finally, according to the parametric study's results, A parametric analysis is done to assess the impact of changing reinforcement ratio, spacing between the ties, inner-to-outer section width ratio, and a comparison with steel reinforcement. The computational results clearly show how an Increased longitudinal GFRP reinforcement ratio improves the columns' bearing capability, but when compared to steel reinforcement, it provides less bearing capability. For the optimum outcome with hollow square concrete columns, it is advised to adopt the limit of the *i/o* between 0.27 and 0.38. In addition, changing the spacing between stirrups was shown not to significantly impact the capacity for axial load in hollow square concrete columns.

Keywords: Hollow columns, square section, compression load, finite element analysis (FEA), Abaqus.

1. INTRODUCTION

Concrete columns with hollow cores are chosen over solid concrete columns for utility poles, ground piles, medium-to-high bridge piers, and the piers of high bridges because they have greater axial loads and bending moment resistance, greater structural effectiveness, high strength-to-mass ratio, reduce self-weight and more affordable styles [1]. These columns are financially possible substitutes for solid concrete bridge pier because they lessen the column's mass's contribution to seismic reaction and the pressure applied on the foundations [2-4]. Additionally, Hollow sections enable higher-quality structural members for reinforced concrete wall piers and bridge columns because the lower hydration heat causes fewer shrinkage cracks. Several studies explore the behavior of concrete hollow columns with steel reinforcement under various types of loading. These studies discovered that the inner-to-outer diameter ratio (*i/o*), longitudinal reinforcement ratio, and axial loading all affect structural performance. Moreover, the ductility of hollow section columns with steel reinforcement decreased when *i/o* was raised while keeping the other variables constant. A brittle failure due to shear happened after the material had reached its maximum capacity, which led to a sudden drop in axial compressive strength. In the case of greater *i/o* ratios, this decrease in compressive strength was more noticeable [5].

Corrosion is becoming a major problem since hollow concrete columns have thinner walls and a smaller concrete cover for the steel reinforcing than solid concrete columns. It minimizes the axial loading capacity by damaging the steel bars of the transverse confinements [6]. Currently, many hollow concrete bridge columns are reinforced and upgraded to ensure they function as planned. As a result, a Non-corroding element is required to overcome the hollow section's constrained axial strengths and stresses. Fiber-reinforced polymers are often used as interior reinforcement and confinement outside the building of new concrete constructions as well as the upgrading and/or strengthening of existing structures [7]. (GFRP) have most recently been employed as transversal and longitudinal reinforcements in solid and hollow sections of concrete columns. The usage of glass fiber reinforced polymers (GFRP) in building projects is expanding as a consequence of its superiority over traditional steel in many ways, including cheap maintenance costs, excellent corrosion resistance, durability, improved fire resistance, and attractive appearance [8].

Mohammed [9] examined the performance of 14 fiber-reinforced full-scale columns under axial loading. Therefore, the type of failure for the columns supposedly occurred of the main bars' buckling when the amount of the transverse reinforcement is reduced (0.7%). However, the collapse of the columns occurred as a consequence of transversal confinement breaking and concrete core crushing at lateral reinforcement ratios (1.5% and 2.7%). GFRP-confined concrete calibration model based on test data and the regression analysis approach to forecasting the specimens' axial capacity and strain suggested by Afifi [10]. Hadi [11] investigated the structural behavior of 12 GFRP-reinforced circular specimens in diameter of (205) mm and (800) mm in height under various types of loading. It was discovered that GFRP-RC specimens' moment and axial loading

capacities were lower than those of their steel-RC equivalent. Further, when the GFRP bar's axial compression was neglected, a wider gap developed between measurements of the column's axial strength based on theory and experiment. Al Ajarmeh [12] studied the performance of hollow, GFRP-reinforced sectional columns and noted that the amount and diameter of bars enhanced the axial strain, confinement's effectiveness, and axial strength of Hollow columns. The confinement efficiency was raised to 12% by using several GFRP bars with smaller diameters. Furthermore, The Efficiency of confinement was raised to 12% by using several GFRP bars with smaller diameters.

Various researchers investigated solid concrete columns with GFRP reinforcement subjected to varying load situations using finite element modeling (FEM) [13–19]. These studies revealed that FEM properly expected the performance of columns made with fiber-reinforced concrete. The FEM specifically addresses all of the flaws in the numerical simulations. When compared to experiments, Simulations using finite elements save both time and money. by developing computer models that can precisely forecast the complicated destructive behavior of FRP composites. Making certain assumptions is necessary to accelerate finite element simulations and simplify the FEM, but it's also necessary to include real practical testing conditions in FEM. To speed up analysis and improve the precision of numerical predictions, Maintain equilibrium between the types and sizes of parts and the complexity of the modeling. Therefore, the FEM is the most effective instrument for researching engineering issues when it is combined with excellent simulation background knowledge.

All of the earlier research, which was already mentioned, concentrated on studying solid sections in addition to circular hollow sections with GFRP reinforcement. No research has examined columns with hollow square sections. This paper suggests a new FEM model to determine the compressive behavior of hollow-square concrete columns with GFRP reinforcement. ABAQUS was used to construct a FEM model of the suggested column to accomplish this goal. Using experimental data from earlier studies, this model was calibrated for a range of material and specimen geometry characteristics.

2. METHODS

2.1 Finite Element Simulations

Modeling hollow square concrete columns with axial compression load that is mainly applied was done in this work using the 3D finite element program ABAQUS (2019 version). This approach was intended to fully establish the correlation between axial load and axial displacement by loading the modeled column units to their maximum strengths. The next sections provide an overview of the material models and other FEA-specific details.

2.2 Element Types and Boundary Conditions

FEM accuracy is dependent on precise material simulations and experimental boundary conditions. The top end of each column's FEA model was left uncontrolled while an applied evenly distributed axial load was imposed, using the displacement control technique, while the base of each column was constrained for all degrees of freedom (DOF). While creating all FE models, the element types (C3D8R) and (T3D2) were employed. The C3D8R type has eight nodes in a continuum of three dimensions and three DOF for translation for all nodes. The concrete, bearing plate, and collar were modeled in this element. The other type of element is called T3D2, a two-noded truss in three dimensions with three translational DOF for each node. The longitudinal bars and stirrups were modeled using this element. The constraint on "embedded regions" is a function of ABAQUS for defining the interaction relationship between the GFRP and the concrete materials. It links the compatible (DOF) of the reinforcing bar truss components to the essential DOF of concrete's three-dimensional stress elements. All elements have a mesh size of 20 mm. Figure 1 presents a detailed view of the simulated models.

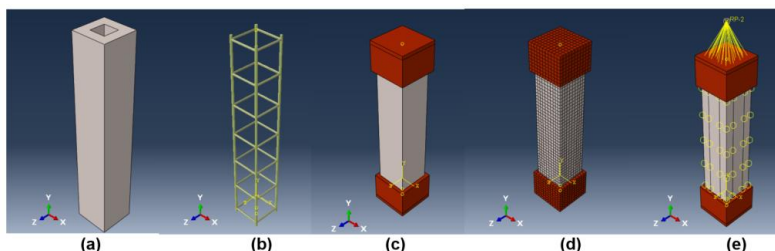


Figure 1: FEA details (a) Column, (b) Reinforcement-cage, (c) Steel plate and collar, (d) Elements with a mesh size of 20 mm, and (e) Applied load and interaction.

2.3 Materials Models

Due to the complexity of the material, simulating concrete's behavior is a difficult challenge. The present work employed concrete with 30 MPa of compressive strength, Young modulus, and Poisson ratio were used

as two factors to imitate the concrete behaviors. Young's modulus was determined Using the Equation given by Equation [1], given a Poisson's ratio value of 0.2 [13].

$$E_c = 4700\sqrt{f'_c} \tag{1}$$

Where f'_c is the concrete's compressive strength at the 28-day test.

In ABAQUS, several models are offered, including the Drucker-Prager, concrete-damaged plasticity, brittle cracking, and smeared cracked models. The present study simulated concrete's inelastic behavior using the concrete damaged plasticity model (CDPM). Considering concrete's cracking and crushing, this model can depict the material's complicated character. Therefore, it is often used to simulate the nonlinearity of concrete. Figure 2 illustrates how the CDPM takes into account the specification of several concrete qualities, including plasticity, tensile, compressive, and destructive behavior [15].

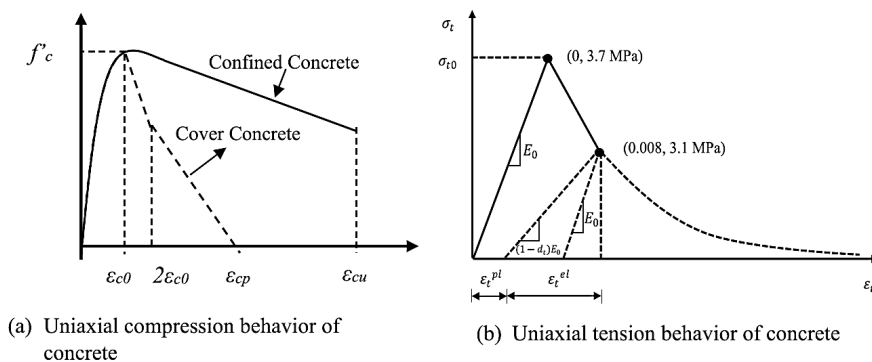


Figure 2: Concrete material model used in ABAQUS.

Based on the ABAQUS 2019 user guide, concrete's plastic behavior considers the following five concrete parameters displayed in Table 1.

Table 1: Concrete's plastic behavior characteristics in Abaqus.

Parameter	dilation angle (Ψ)	Eccentricity (ε)	biaxial to uniaxial stresses (fb0/fc0)	shape factor (K)	Viscosity (μ)
Value	31.5	0.1	1.165	0.6667	0

Concrete Damaged Plastic (CDP) is typically chosen for studies like this one because it covers a wide range of concrete's nonlinear inelastic behavior in three dimensions, involving confinement and damaging approaches as well as characteristics in the inelastic range for compression, tension, and plasticity [15, 16] and simulating the GFRP bars' behavior up to failure by considering them as a linear elastic substance that is isotropic. Two factors were used to determine the elastic behavior of GFRP bars: the elasticity modulus, which was set at 50,000 MPa, and the Poisson's ratio, which was set at 0.25. Assuming the same elastic modulus, it was determined that GFRP bars' compressive strength was equal to 50% of the tensile strength, which was the tensile strength set as 850 MPa [17]. The details and properties of reinforcement bars are shown in Table 2.

Table 2: Properties of reinforcement.

Reinforcement type	Modulus of elasticity (MPa)	Tensile strength (MPa)
GFRP	50,000	850
STEEL	200,000	420

2.4 Validation of Selected FEM

GFRP-reinforced concrete column unit G-0 evaluated by F. Abed et al. [20] was used to confirm the validity of the computational approach. A column with a 180 mm-square cross section on each side is made up. The column was 1000 mm high and loaded concentrically. It was fixed at 27.5 mm of clear concrete cover. Four 16 mm diameter bars were used to strengthen columns, with a 2.48% longitudinal reinforcement ratio as a result, and had 180 mm-diameter steel ties placed 180 mm apart that were transversely strengthened. To prevent sudden failure, The columns' ends had a reduction in the spacing of the stirrup to 35 mm. In Figure 3, a comparison of the test outcomes and the computed average axial load-displacement responses of the concrete column from the FEM is shown. In general, the FE responses and measured responses match well For both

the peak load and the softer part of the descending part. These similarities provided additional evidence that the modeling and material approach models accurately depict concrete columns' compression capacity.

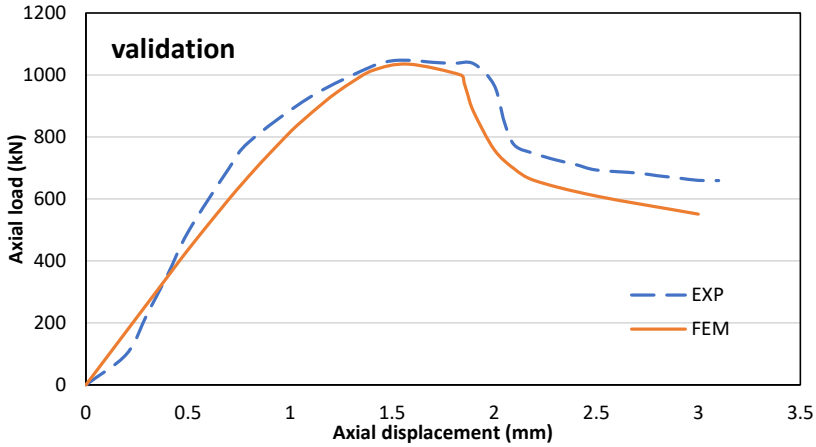


Figure 3: The load-displacement curve for specimen G-0.

2.5 Model Formulation

Twelve specimens, separated into three groups of concrete hollow square columns with GFRP reinforcement bars and one group of steel reinforcement bars, were simulated in ABAQUS under axial compression load. All of the columns selected for the studies had an outside section width of 180 mm, and the hollow dimension was determined using a range of preselected inner to outer i/o section width values between 0.28 and 0.5. The columns were supposed to be 900 mm in height. Table 3 shows the simulated columns' geometrical characteristics.

Table 3: Details of simulated columns.

Group no.	Specimen label	Reinforcement type	Internal long. reinforcement	Spacing between ties (mm)	Hollow size (mm)	Axial load (kN)	Axial displacement (mm)
Group 1	G1	GFRP	4Ø12	@150	80x80	798.1	1.79
	G2		8Ø12			844.9	1.87
	G3		12Ø12			889.7	1.94
Group 2	S1	STEEL	4Ø12	@150	80x80	893.9	1.68
	S2		8Ø12			1143.2	1.98
	S3		12Ø12			1327.2	2.07
Group 3	H1	GFRP	4Ø12	@150	50x50	910.8	1.91
	H2				70x70	852.1	1.68
	H3				90x90	705.9	1.63
Group 4	L1	GFRP	4Ø12	@180	80x80	790.8	1.74
	L2			@160		808.1	1.78
	L3			@140		820.4	1.73

3. DISCUSSIONS OF NUMERICAL RESULTS

3.1 Longitudinal Reinforcement Ratio

Group one includes three specimens that were simulated in Abaqus; each one of these columns has a different reinforcement ratio varied from 1.7 to 5.2. G1 has a 1.7 reinforcement ratio, which is made with 4 bars of 12 mm, and shows an axial load capacity equal to 798 kN with 1.9 mm axial displacement. The second specimen, G2, has a 3.4 reinforcement ratio with 8 bars of 12 mm, and the result shows it has 845 Kn axial load and 1.8 mm axial capacity, which has increased in axial capacity by 5.89 % concerning the first specimen G1 and a decrease in axial displacement by 5.26 %. Third specimen G3 has 889 kN axial loads and 1.95 mm axial displacement, with an 11.4 % increase in axial load capacity and a 2.63 % increase in axial displacement to G1. All data of these columns are shown in Figure 4.

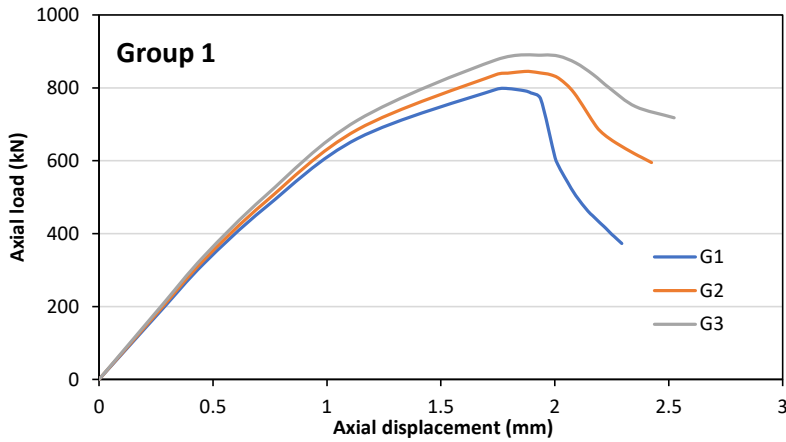


Figure 4: The load-displacement curve for Group 1.

The behavior of previous specimens exhibited similar phenomena according to the failure pattern, as it is clear that the failure in all these columns and the appearance of cracks is in the central region of the column, which indicates the occurrence of compression failure, as shown in Figure 5.

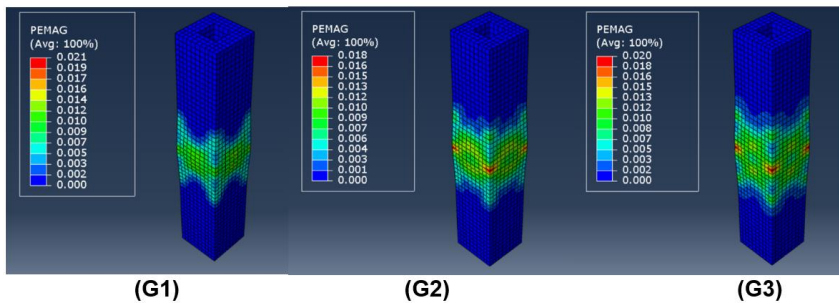


Figure 5: PEMAG for group 1.

3.2 Ties Spacing

To study the effect of spacing between ties, group four, which includes three hollow square columns, was simulated with different spacing of 140 mm, 160 mm, and 180 mm for specimens L1, L2, and L3, respectively. According to the result shown in Figure 6, all of these columns have almost the same axial load, which led to the changing of the spacing between GFRP ties in the hollow square column, having no significant effects on the column's axial load capacity. Also, the axial displacement in these three columns is about the same.

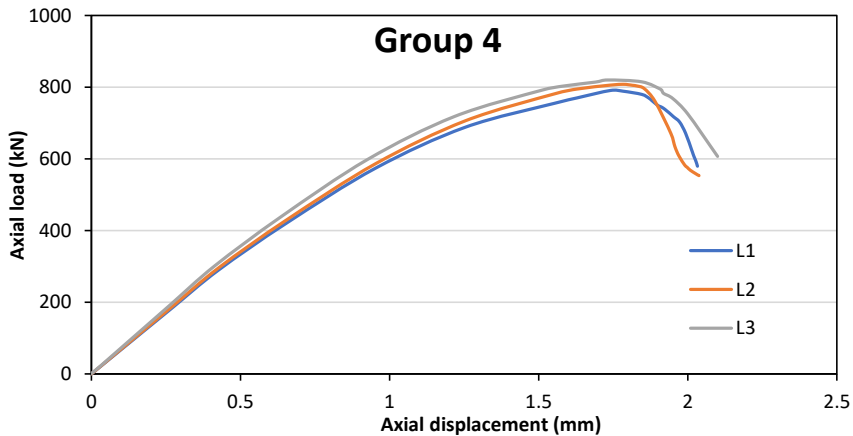


Figure 6: The load-displacement curve for Group 4.

On the other hand, each column has a different crack pattern, as shown in Figure 7. L1, which has spaced between stirrup equal to 180 mm, the cracks distributed along the faces of the column; when the spacing between stirrups decreases, the cracks appear closer in the midsection for specimens L2 and L3.

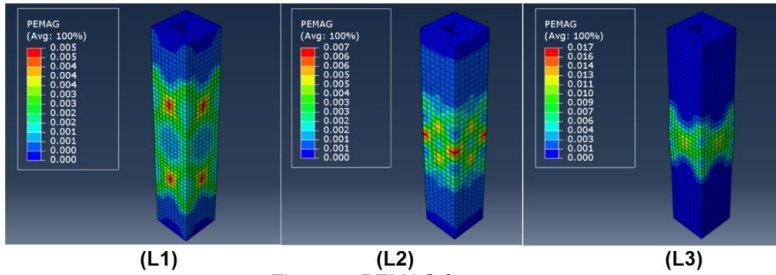


Figure 7: PEMAG for group 4.

3.3 Inner-To-Outer I/O Section Width Ratio

Group 3 consists of three hollow square columns with different *i/o* varied from 0.27 to 0.5. Model H1, which has an *i/o* ratio of 0.27, was made by making the hole dimensions 50 mm; the results of the analysis showed that it has an axial load of 910 kN in addition to an axial displacement of 1.9 mm, while the second model H2 has *i/o* ratio of 0.38 by Making the dimensions of hole 70 mm showed an axial load of 852 kN, which means that it is 37.6% less to the first model. An axial displacement of 1.68 mm is 11.5% less than the first model. For the third model, H3, which has a ratio of 0.5 Through a hole of 90 mm, it showed an axial load value of 706 kN, which means that it is less than the first model by 22.4%, and it also showed axial displacement of 1.62 mm, which is less by 14.7% compared to the first model H 1. All results are shown in Figure 8.

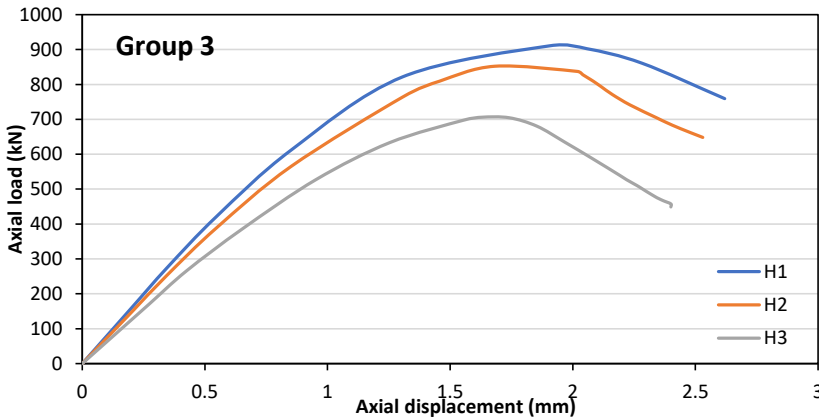


Figure 8: The load-displacement curve for Group 3.

Each column has a crack pattern, as shown in Figure 9. The difference in mechanism for failure of the specimens is a result of the wall thickness of the hollow concrete column, which causes a failure of spalling the concrete cover.

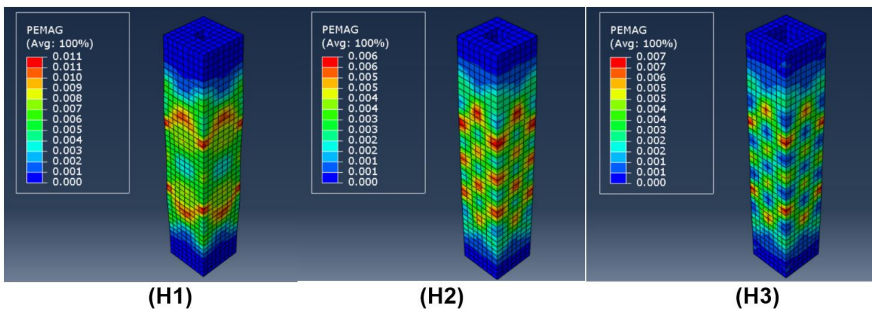


Figure 9: PEMAG for group 3.

3.4 Comparison between GFRP and Steel Reinforcement

The second group included three hollow square columns that were established the same as the first group, with details and dimensions, but with a different type of reinforcement, where reinforcing steel was used instead of GFRP reinforcement, in order to compare the two types of reinforcement and know the structural behavior of each of them and its impact on behavior compression of the hollow square concrete column. For a 1.7 reinforcement ratio, model S1 was simulated, and it showed an axial load of 894 kN, which is greater by 12.03% than model G1. and the axial displacement of model S1 is 1.68mm, which is lower than model G1 by 6.15% as shown in Figure 10. For the 3.47 reinforcement ratio, model S2 was simulated, and the FEM results show it has an axial load of 1143 kN, which is 35.3% more than model G2. Both of these models have an almost similar axial displacement value, shown in Figure 11. Lastly, for the 5.2 reinforcement ratio, model S3 was simulated and showed an axial load of 1327 KN with an increase of 49.3% concerning model G3. Also, both columns have an almost similar result in axial displacement, as shown in Figure 12.

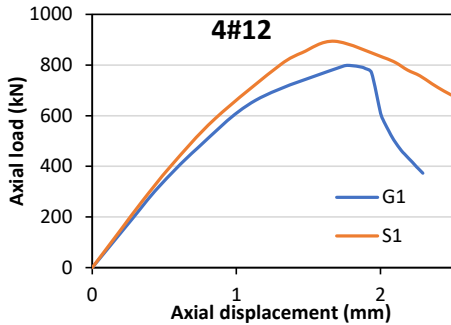


Figure 10: Load-displacement curve for specimens G1 and S1.

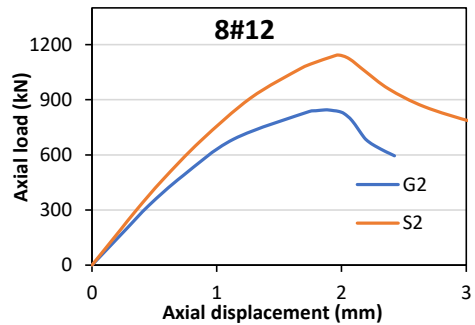


Figure 11: Load-displacement curve for specimens G2 and S2.

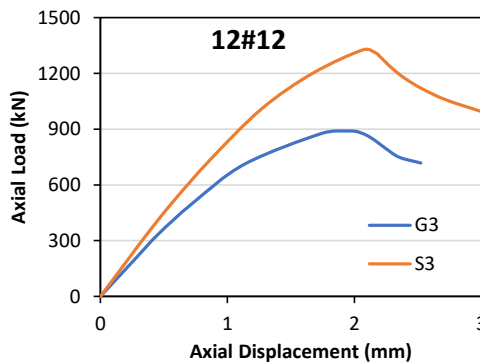


Figure 12: Load-displacement curve for specimens G3 and S3.

4. CONCLUSIONS

To investigate the behavior of GFRP-reinforced hollow square concrete columns for axial compression load, axial loading tests were carried out on twelve-column specimens and were conducted using a verified model on Abaqus software. The effects of reinforcement ratio, reinforcement type, tie spacing, and i/o ratio on the compression behavior of these specimens were investigated, and the outcomes were obtained. Here are many important conclusions that may be drawn:

- The concrete square hollow GFRP columns numerical simulation model according to the CDPM, and the linear elastic behavior of GFRP produces results that are comparable to those of the experiment. As a result, the suggested column simulation approach is trustworthy and suitable for parametric research.
- The load-carrying capability of columns is considerably impacted by increasing the reinforcing ratio of GFRP bars, thus obtaining better efficiency. The first model G1, has a 1.7 reinforcement ratio and shows an axial load capacity equal to 798 kN. The two other models have a reinforcement ratio of 3.4

for model G2 and 5.2 for model G3, which has increased by 5.89% and 11.4%, respectively, in axial load capacity concerning the first model G1.

- The effect of changing the distance between the stirrups does not greatly affect the bearing of the column for axial loads but showed a difference in the form of failure when the distance decreased from 180 mm to 140 mm, and this is due to the occurrence of a buckling failure in the GFRP longitudinal bars.
- As it is clear, changing the *i/o* ratio has a clear impact on the behavior of the hollow square concrete columns; therefore, the lower the *i/o*, the less the column bears the axial forces, as well as the appearance of cracks faster, due to small thickness of the concrete wall.
- The GFRP reinforcement shows less axial load capacity for the same volumetric reinforcement ratio than the steel reinforcement. For a 1.7 reinforcement ratio, the steel reinforcement is greater by 12.03% than GFRP reinforcement by mean of the axial capacity, and for the other reinforcement ratios, 3.4 and 5.2 are greater than GFRP reinforcement by 35.3% and 49.3%, respectively.
- According to the research, the ductility is reduced when the steel reinforcement is replaced by GFRP bars.
- The capability of GFRP bars to withstand applied compression forces is less than their ability to withstand tensile forces because GFRP has a lower modulus of elasticity than reinforcing steel bars.

REFERENCES

- [1] Hadi MN, L.e, TD. Behavior of hollow square reinforced concrete column wrapping with CFRP with different fibres orientation. *Constructions and Building Material*. 2014 Jan 15; 50(1): 62-73.
- [2] Hoshikoma JI, Priestley MJ. Flexural behavior of circular hollow column with a single layer of reinforcements under seismic loadings. 2000.
- [3] Abaas RM, Awazli AG. Behavior of Reinforced Concrete Column Subjected to Axial Load and Cyclic Lateral Loads. *jcoeng [Internet]*. 2017 Jan. 31; 23(2): 21-40.
- [4] Ali NK, Salahaldin AI, Hamza AJ. Impact Analysis of Reinforced Concrete Columns with Side Openings Subjected to Eccentric Axial Loads. *Journal of Engineering*. 2015 Feb 1;21(2):1-9.
- [5] Casesse P, De Risi MT, Verderrame GM. A degrading modeling for RC column with hollow cross sections. 2019; 17(8): 1241-1259.
- [6] Zeng JJ, Lv. gF, Lin G, Gio YC, Li LJ. Compressive behaviour of double tubes concrete column with outer square FRPs tube and inner circular high strength steel tubes. *Constructions and Buildings Materials*. 2018 Sep 30; 184(1): 668-680.
- [7] HADI, Muhammad NS; YOUSSEF, Jim. Experimental investigation of GFRP-reinforced and GFRP-encased square concrete specimens under axial and eccentric load, and four-point bending test. *Journal of Composites for Construction*. 2016; 20(5): 04016020.
- [8] Elchallakani M, Karech A, Dung. M, Ali MM, Yong B. Experimental and finite element analysis of GFRP reinforced geopolymer concrete rectangle column subjected to concentric and eccentric axial load. 2018 Jun 1; 14(1): 273-289.
- [9] Mohammed H.M, Afifi. M.Z, Benmokrune B. Performance of concrete column reinforced longitudinally with FRPs bar and confined with FRPs hoop and spiral under axial loading. *Bridge Engineering*. 2014 Jul 1; 19(7): 04014020.
- [10] Afifi M.Z, Mohammed H.M, Benmokrune B. Theoretical stress strain model for circular concrete column confined by GFRP spiral and hoop. 2015 Nov 1; 102(1): 202-213.
- [11] HADI, Muhammad NS; KARIM, Hogr; SHEIKH, M. Neaz. Experimental investigations on circular concrete columns reinforced with GFRP bars and helices under different loading conditions. *Journal of Composites for Construction*. 2016; 20(4).
- [12] AlAjarmeh O.S, Manulo. A.C, Benmokrune B, Karunacena W, Mendes, P. Axial performance of hollow concrete column reinforced with GFRP composite bar with different reinforcement ratio. *Composite Structure*. 2019 Apr 1; 213(1):153-164.
- [13] Dong M, Lokugie W, Elchalakuni M, Karech A. Modelling glass fibre reinforced polymers reinforced geopolymer concrete column. *InStructure*. 2019 Aug 1; 20(1): 813-821.
- [14] Zakaria AW, Al-Baghdadi H. Experimental and numerical study on CFRP-confined square concrete compression members subjected to compressive loading. *Journal of Engineering*. 2020 Mar 23;26(4):141-60.
- [15] Alfarah B, Lopez-Almonsa F, Oler. S. New methodology for calculating damages variable evolutions in Plastic Damage Model for RC structure. *Engineering Structure*. 2017 Feb 1; 132(1): 70-86.
- [16] Hany NF, Hantoeche EG, Harajji M.H. Finite element model of FRPs-confined concrete using modified concrete damaged plasticity. *Engineering Structure*. 2016 Oct 15; 125(1): 1-4.
- [17] Raza A, Ahmed A. Numerical investigations of load-carrying capacity of GFRP- reinforced rectangular concrete member using CDP model in ABAQUS. *Advanced in Civil Engineering*. 2019.
- [18] AL-Shaarbaf I.A, Allawi A.A, Al-Salim N.H. Strength of Reinforced Concrete Column with Transverse Opening. *jcoeng [Internet]*. 2017 Oct. 1; 23(10): 114-133.

- [19] Ibrahim. AM, Fahmy. MF, Wi Z. 3D finite element model of bond controlled behaviour of steel and basalts FRPs-reinforced concrete square bridges column under lateral load. *Composite Structure*. 2016 May 20;143(1): 33-52.
- [20] Abed F, Refai AE, ElMesalami N. Compressive Behaviour of Glass Fiber Reinforced Polymer (GFRP) Reinforced Concrete Columns. *International Conference on Fibre-Reinforced Polymers (FRPs) Composite in Civil Engineering*. Springer, Cham. 2021.